On the Surface of Clouds

SZYMON P. MALINOWSKI* AND ISZTAR ZAWADZKI

Université du Québec à Montreal, Quebec, Canada

(Manuscript received 30 September 1991, in final form 27 January 1992)

ABSTRACT

The cloud–environment mixing process is considered in terms of fractal properties of the cloud–clear air interface. The fractal dimension of the cloud surface is estimated from high-resolution airborne data. The value obtained is $D = 2.55$ in a range of scales from at least 10 m to over 1000 m with the possibility of even greater extension. This differs significantly from values obtained in shear-generated, well-developed, and homogeneous turbulence. The distribution of filament sizes of cloudy and clear air and estimates of the cloud surface and characteristic time of mixing process are given.

1. Introduction

The entrainment of environmental air into a cloud and the following mixing with the cloudy air is a process that crucially influences both cloud dynamics and microphysics. A great number of theoretical and experimental investigations aimed at describing and understanding its physics has been undertaken recently. Our understanding of this process is still far from complete, however, and such basic questions as the time dependence of the process, its efficiency, and the influence of the driving mechanism on the development of turbulence (e.g., shear versus convective generation) remain unanswered. The relatively new fractal geometry approach to the description of turbulent flows may be helpful and the discussion given here focuses these questions in light of the recent theoretical and observational additions to the understanding of this complex problem. We investigate the fractal properties of the cloud–clear air interface and compare the results to the interfaces in well-developed turbulence in shear flows. We argue that in-cloud turbulence may differ significantly from the latter.

The observational evidence indicates that two kinds of cumulus cloud volumes can be identified:

1) homogeneous with respect to the high-resolution Forward Scattering Spectrometer Probe (FSSP) sampling, correlated usually with positive upward velocity;
2) nonhomogeneous, with high variations of LWC and droplet population as well as other thermodynamic and dynamic parameters (e.g., see Austin et al. 1985).

It seems that in some parts of the cloud volume the intensive entrainment and turbulent mixing take place, while other parts contain either unmixed air raised from lower levels, or air mixed to the scales below the resolution of observational data. Findings of Paluch and Baumgardner (1989) indicate that the inhomogeneities at the cloud–environment border may be treated as filaments of cloudy and clear air of various sizes nonuniformly distributed in space. This is consistent with the characteristics of fractal objects. One may call it the "clustering" of the entrainment–mixing process, thus looking for scaling and fractal properties of the clusters is a natural approach to such phenomena.

This paper is organized as follows. In section 2 a brief outline of the fractal approach to describe mixing and entrainment in shear flows is given. Section 3 describes high-resolution FSSP measurements used to determine the fractal dimension of the cloud–clear air interface. From this, estimates are given of the characteristic mixing time and of the area of the cloud–environment interface. The differences between fractal properties of surfaces in shear-generated turbulence and cloud–clear air interface as well as consequences for the understanding of the entrainment–mixing process in clouds are discussed and summarized in the last section.

2. Mixing and entrainment in shear flows

In the late 1970s a number of papers describing turbulent mixing experiments in shear layers and jets appeared (e.g., Brown and Roshko 1974; Broadwell and Breidenthal 1982, hereafter referred to as BB). Broadwell and Breidenthal summarized the experimental

* On leave from University of Warsaw, Institute of Geophysics.

Corresponding author address: Dr. Isztar Zawadzki, Université du Québec a Montreal, Case Postale 8888, Succursale A, Montreal, H3C 3P8 Quebec, Canada.

evidence proposing the following description of mixing in the turbulent shear layers.

Mixing takes place in a series of events. Each mixing event begins with the large-scale engulfment sweeping the fluid from both sides of the shear layer into localized regions. The initially large-scale filaments of the two fluids undergo breaking down toward smaller scales due to the action of turbulence. Turbulence also stretches the interface between the fluids and enhances the molecular diffusion across the increasing surface. Based on this picture of mixing BB estimated the time in which the interface is stretched to the smallest possible scale of convolutions (Kolmogorov scale). Adopting some heuristic reasoning they estimated also the final surface of the interface and argued that the time necessary to complete the mixing due to molecular diffusion through this interface is negligibly small. This model has been used by Jensen and Baker (1989) as a basis for description of the cloud–environment mixing.

Two papers by researchers from Yale University (Sreenivasan et al. 1989a; Sreenivasan et al. 1989b, hereafter referred to as SRM and SPMR, respectively) give an estimation of the interface surface, based on experimental evidence in various kinds of shear-generated turbulence and on theoretical considerations, that is different from the one given by BB. For the reader's convenience some main points of their research are summarized.

a. *Fractal dimension of the surfaces in turbulent flows*

In their papers, SRM and SPMR analyze the visualized surface of the constant concentration of a passive scalar in different kinds of well-developed turbulent flows (such as turbulent jets, shear layers, and boundary layers). From this analysis they obtain the fractal dimension of the surface. The spatial resolution of the analyzed 1D and 2D sections through the flows is close to the Kolmogorov scale, so that the convolutions of the surface due to all acting dynamic scales of turbulent eddies can be observed. The obtained fractal dimension, D, of the surfaces in all of the experiments is 2.35 $\pm$ 0.05. They show that this is in very good agreement with theoretical prediction based on the assumptions of Reynolds number similarity and constant turbulent energy flux down to the Kolmogorov scale. The molecular dissipation is considered as acting only in the smallest eddies (of about the Kolmogorov scale). The theoretical prediction gives $D = 7/3$ when intermittence of the turbulent energy dissipation is not taken into account and $D \approx 2.36$ when it is taken into account.

Fractal dimension alone, although giving a rough idea of how much of the surface is convoluted and how it fills three-dimensional volume, is not sufficient to estimate the surface of the interface. If the interface is a "true" fractal, with all possible scales from infinity to 0, its surface would be infinite. Of course this is not the case. Since the turbulence is generated at some scale and the inertial range of the eddies has a truncation at about the Kolmogorov scale, the interface is finite and has fractal properties only within this range of scales. This allows us to calculate the real surface S_F of the interface from the SRM expression:

$$S_F = S_0[L/\eta]^{D-2}, \tag{1}$$

where S_0 is the surface measured with resolution L (initial surface of the mixing event of size L) and η is the Kolmogorov scale. This is the real interface across which the molecular exchange occurs. SRM estimate the momentum flux through this surface as

$$M_F = \alpha S_F U_c^2, \tag{2}$$

where α is some constant and U_c is the characteristic velocity of the flow. Comparing this with the momentum flux entrained by turbulent flow:

$$M_F = S_p V_e U_c, \tag{3}$$

where S_p is the surface through which entrainment occurs—some average surface of the flow—and V_e is entrainment velocity per unit surface. Then

$$\frac{V_e}{U_c} = \beta, \tag{4}$$

where $\beta = \alpha S_0/S_p$ is constant for a given flow. Note that β contains information about the size of the largest eddies, the Kolmogorov scale η, and the ratio S_0/S_p. Since η can be related to the viscosity coefficient ν and the turbulent energy flux ϵ by $\eta = \nu^{3/4}\epsilon^{1/4}$ only the geometry of the flow, determined by external flow forcing and molecular viscosity, governs the entrainment. It should be pointed out that Eq. (4), being the result of calculations based on assumptions of existence of the inertial range of eddies and Reynolds number similarity, is the same as the well-known Taylor entrainment hypothesis widely adopted to estimate entrainment into various geophysical turbulent flows (for an extended review see Turner 1986).

b. *Direct application of SRM theory to cloud–environment mixing*

The SRM results are obtained for well-developed turbulent flows with a well-defined source of turbulent energy (shear). When adopting them to the cloud physics a number of general questions arise: Is the turbulence within clouds well developed? What are its sources? From analysis of numerical simulations of clouds at high resolutions, Grabowski and Clark (1991) conclude that in convective clouds entraining eddies are driven by baroclinicity at the cloud–environment interface. This may lead to a kind of turbulence different from the one in jets or shear layers. On the other hand, the measurements of the turbulent energy spec-

trum in cumulus (MacPherson and Isaac 1977; MacPherson 1979) are in good agreement with the $^5/_3$ power law; that is, the Kolmogorov theory seems to be applicable. These studies lead to the following picture of the entrainment–mixing process in clouds.

The entrainment–mixing occurs in a series of events. Each event of cloud and clear-air mixing is initiated by the development of engulfment at a cloud boundary due to baroclinic instability; the following engulfments of the smaller scale lead to convolutions at smaller and smaller scales, from the scale of the initial engulfment to the Kolmogorov scale. If the fall of the cloud droplets through clear-air filaments is neglected, mixing is completed by the action of molecular diffusion through the stretched cloudy air–clear air interface. This picture agrees very well with description of SRM. The volume of cloudy air in cloudy filaments is maintained during the folding process and the total volume containing some cloudy air depends on the proportion into which clear-air filaments are incorporated between the filaments of cloudy air. Deep updrafts and penetrative downdrafts within a developed cloud extend further the cloud–clear air interface at which the described mixing process occurs.

Let us consider the single mixing event as previously mentioned, that is, the development of the convective cloudy filament that originates engulfment of the interface, followed by the excitations of the smaller eddies, down to the Kolmogorov scale, and finally the molecular exchange through established interface. The initial size of engulfment and the turbulent energy given to the mixing event (and then dissipated) are enough to estimate the mixing time and length scales. Assume that the characteristic length of the mixing event is L and the corresponding initial surface is

$$S_0 = aL^2, \tag{5}$$

where a is some constant depending on the shape of initial engulfment. From (1) we can estimate the final surface S_F as

$$S_F = aL^D\eta^{2-D}. \tag{6}$$

During the surface growth, the thickness of the layer separating the two fluids remains the same and is of order of η (SRM). The boundary volume V_m

$$V_m = \eta S_F = aL^D\eta^{3-D}, \tag{7}$$

may be treated as mixed, while the whole volume of the mixing event may be expressed as

$$V_v = bL^3; \tag{8}$$

where b is constant, again depending on the shape of the initial engulfment. The time necessary to complete this phase of mixing may be estimated after BB as

$$t_1 = \frac{L^{2/3} - \eta^{2/3}}{2/3c\epsilon^{1/3}}, \tag{9}$$

where c is constant and ϵ is turbulent energy dissipation rate. We can define some characteristic thickness of the filaments of the cloudy and environmental air as

$$L_f = V_v/S_F = L^{3-D}\eta^{D-2}d; \quad d = b/a. \tag{10}$$

In making the last step one should keep in mind that, since the separating surface has a fractal nature, filaments of all sizes from the Kolmogorov scale to nearly L exist in the beginning of the second phase of mixing. Our ability to define a characteristic thickness of the filaments stems from the truncation of the scaling properties of the flow at both ends of the scale. Furthermore, the fact that the whole range of eddies has been developed does not mean that the size of all of the filaments is of the order of Kolmogorov scale. In this respect the ideas developed by BB differ from the fractal approach to the problem.

The estimate of the time necessary to complete the second phase of mixing, that is, the molecular diffusion across the interface established by turbulent mixing, can be obtained now from the relation:

$$t_2 = L_f^2/\nu. \tag{11}$$

We should note the extreme sensitivity of L_f and t_2 to the value of fractal dimension. In effect, when η is of order of 10^{-3} m and L of order of 100 m, for a cloud surface in the three-dimensional Euclidean space L_f and t_2 may vary within a range of four and eight orders of magnitude, respectively, with D going from 2 to 3.

Let us evaluate now η, S_F/S_0 (the increase in interface surface due to turbulent mixing), V_m/V_v (the fraction of the volume truly mixed by viscous forces in the first phase of mixing), t_1 and t_2 (the characteristic time of the first and second phase of mixing, respectively), and L_f (the characteristic thickness of filaments). For this we must assume some values for the constants in (5) to (11). Consider the initial shape of the cloudy bubble to be semispherical. Thus, $a \sim 1.5$, and if the mixed parcel contains as much clear air as original cloudy air (later we will see that there is some experimental evidence to this effect), then b/a is of order of unity. Following BB, we will take $c \sim 1$ as well. With this we give in Table 1 the estimates of the various parameters for three values of ϵ and two values of the fractal dimension of the cloud surface. Values of ϵ equal to 10, 100, and 1000 cm^2 s^{-3} are chosen as characteristic for low, medium, and high turbulent energy dissipation rates observed within cumulus clouds (MacPherson 1979). The initial size of the convective cloudy bubble taken as L = 100 m (10^4 cm) is, according to Grabowski and Clark (1991), the characteristic size of the cloud-boundary engulfment. For first phase of the entrainment–mixing process, lasting one to three minutes, nearly no "real" mixing occurs! Additionally we note that for $D = ^7/_3$ t_2 has unrealistically high values, of order of several days. This leads to the conclusion that a fractal dimension obtained from shear-generated turbulence is not satisfactory for de-

TABLE 1. Estimated characteristics of cloud–environment mixing processes for $D = 2.33$ (7/3 as in SRM) and $D = 2.55$ (obtained in our study) and for $L = 100$ m. Symbols are ϵ: turbulent energy dissipation rate, η: Kolmogorov scale, S_F/S_0: increment of cloud surface due to stretching by turbulence, V_M/V_0: ratio of the mixed volume in the first phase of the entrainment–mixing process to the initial volume of air undergoing the entrainment–mixing process, t_1: characteristic time of the first phase of the entrainment–mixing process, L_f: characteristic size of filaments formed in the first phase of the entrainment–mixing process, t_2: characteristic time of the second phase of the entrainment–mixing process.

		S_F/S_0		$V_M/V_0 \times 10^{-3}$			L_f(cm)		t_2 (h)	
ϵ (cm^2 s^{-3})	η (cm)	$D = 2.33$	$D = 2.55$	$D = 2.33$	$D = 2.55$	t_1 (s)	$D = 2.33$	$D = 2.55$	$D = 2.33$	$D = 2.55$
10^1	.136	41.9	475	.57	6.5	215	239	21.1	106	.82
10^2	.076	50.9	654	.39	5.0	100	197	15.3	72	.43
10^3	.043	61.5	895	.26	3.8	46.4	163	11.2	49	.23

scribing the cloud–environment entrainment and mixing.

3. Fractal dimension of the cloud surface

a. Literature review

After Mandelbrot (1982) the following procedure may often be adopted in isotropic cases for obtaining fractal dimension of the set from its cross sections: If D_N is the fractal dimension of the N-dimensional section of the fractal set embedded in M-dimensional space ($M > N$), one can obtain fractal dimension of the set from:

$$D = D_N + (M - N). \tag{12}$$

Unfortunately, cloud cross sections of the quality and the resolution necessary for the analysis of fractal properties of the cloud surfaces are not available yet. On the other hand, satellite images of clouds that are not cross sections but rather horizontal projections of cloud surfaces are abundant. Assuming that (12) is valid for projections as well, some papers aimed at determining the fractal dimension of the cloud surface appeared in recent years. Probably the best known is Lovejoy's (1982) report of the radar and satellite images of the tropical cloud systems. The fractal dimension D_2 of the cloud–environment interface obtained from perimeter–area relation is estimated as 1.35 (this corresponds to $D = 2.35$) for the range of scales from about 1 km to over 1000 km. This result is surprisingly consistent with SRM findings. However, Gifford (1989) argues that a reexamination of Lovejoy's data gives an estimation of fractal dimension equal to 2.77 for scales over several hundreds of kilometers. According to Gifford, this is consistent with the change of the character of the atmospheric turbulence from 3D to 2D in these scales, manifested by change of the turbulent energy spectrum from $k^{-5/3}$ to k^{-3}. Carter et al. (1986), using a different method based on radiance measurements of the individual cumulus clouds, arrive a number of 1.16 for D_2, generally for smaller scales than Lovejoy (1982). Based on a study of perimeter–area relationship applied to high-resolution satellite images, Cahalan and Joseph (1989, hereafter referred to as CJ) estimated D_2 in the range 1.29–1.62, varying with cloud types and sizes. For fair-weather cumuli their estimation of D_2 is about 1.3 for clouds smaller than 500 m in diameter and about 1.55 for clouds of larger diameters.

b. The experimental data

Virtually all previous attempts to estimate the fractal dimension of the cloud surface were based on perimeter–area relation on satellite or radar pictures. A different point of view about cloud–environment interface can be obtained from FSSP data from several small cumulus penetrations made during EMFS (Eulerian Model Evaluation Field Study), an experiment performed at North Bay, Ontario, in spring 1990. For the purpose of this study only data on total droplet strobe counts and LWC from two experimental flights (42B, 27 April 1990 and 44A, 29 April 1990) were selected. The 64-Hz data were recorded on board the Environment Canada Twin Otter aircraft flying at constant altitude with a constant course and true airspeed of about 68 m s^{-1}. Thus, the spatial resolution of the data is slightly above 1 m. Total lengths of the records are 126 144 and 44 984 samples for flights 42B and 44A, respectively. Over 17 small cumulus clouds were penetrated in flight 42B and about 10 in flight 42A; however, data were not separated and the following analyses were performed on the whole length of the data records. Generally, penetrations were made about 300 m below tops of shallow, fair weather cumulus clouds. Observed 64-Hz maximum values of LWC (liquid water content) were 1.1 g m^{-3} and 0.8 g m^{-3} for flights 42B and 44A, respectively. Maximum total droplet concentration was about 650 cm^{-3} in both flights. In the following analyses the direct output from FSSP, the total droplet count (TDC), will be used (650 cm^{-3} droplet concentration corresponds to TDC $\approx$ 250).

An example of the records from part of one cloud penetration is given in Fig. 1. On the left-hand side of the figure (samples 700–950) there is a cross section of an unmixed part of the cloud. The LWC is close to adiabatic values as estimated from the sounding; the TDC reaches maximum observed values. Very rapid

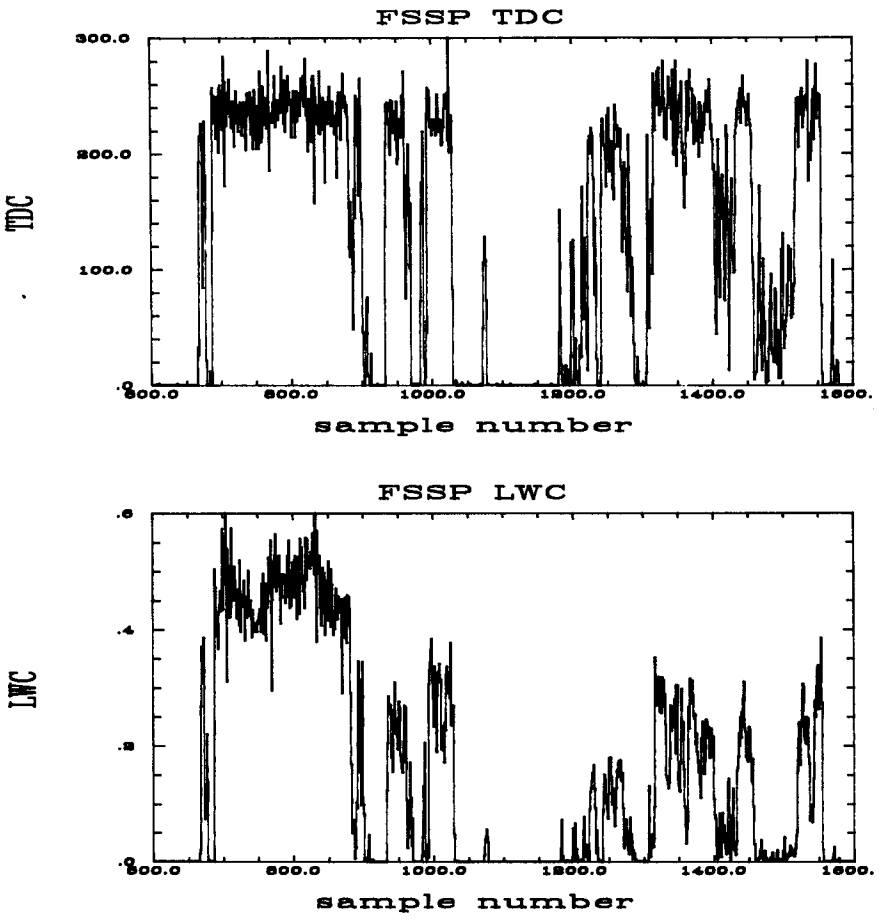

FIG. 1. An example of 64-Hz FSSP records from one of the cloud penetrations during flight 44A. (a) Total droplets count (TDC). (b) LWC (g m^{-3}).

changes of TDC from zero to a certain maximum level are a characteristic feature of the remaining part of the record. A similar feature with additional variability of the "maximum level" represents the right-hand side of the LWC record. This difference in the behavior of TDC and LWC records may be explained by the more conservative nature of TDC during evaporation. Both records strongly support findings of Paluch and Baumgardner (1989) about the convoluted nature of the cloud–clear air interface.

c. *Method of the analysis*

The main purpose of our data analysis is to estimate the fractal dimension of the cloud–environment interface in the range of scales covered by experimental data. For this purpose the following procedure was adopted.

The data records are treated as 1D (line) sections across the field of small cumulus clouds. Each record consists of the consecutive segments of data from penetrations through clear and cloudy filaments. Cloudy segments are defined as record segments at which the value (TDC or LWC) is over a certain threshold. Points on the beginning of the consecutive cloudy and clear segments correspond to the intersection of the line flight and the cloud surface. This set of points is analogous to a Cantor set. For each flight several such sets were obtained. In the following, results for the threshold values $N_t = 10$ and $N_t = 150$ for TDC as well as $L_t = 0.1$ g m^{-3} and $L_t = 0.5$ g m^{-3} for LWC are presented. The cumulative length-distribution analysis is given only for TDC data and $N_t = 10$.

Let us first consider the cumulative distribution of lengths of cloudy and clear-air segments and compare this to the results of similar measurements reported by Duroure and Guillemet (1990). For $N_t = 10$ the number S of cloudy (clear) air segments of length $> R$ versus R were plotted on log–log plot (Fig. 2). As can be seen, for a statistically significant amount of segments ($S > 15$), the experimental points for both cloudy and clear air segments lay close to straight lines, in qualitative agreement with Duroure and Guillemet (1990). The slope of all of the lines is in the range

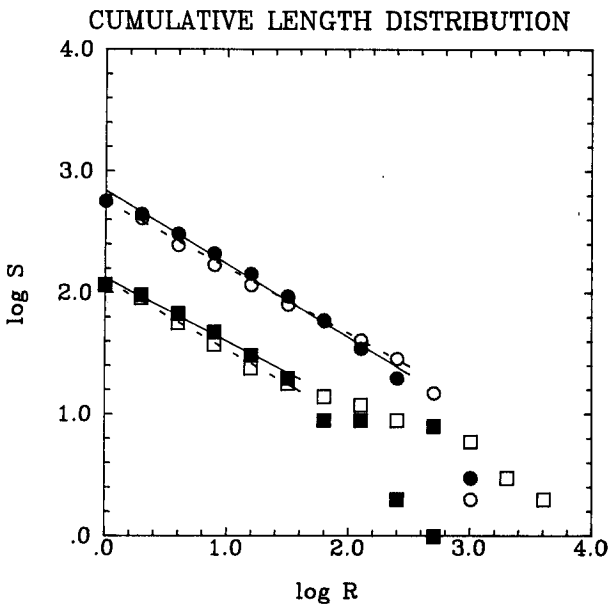

FIG. 2. Cumulative length distribution of clear (empty marks) and cloudy (filled marks) segments determined by TDC threshold N_t = 10. Circles correspond to flight 42B, squares to flight 44A. Best fit to the points representing statistically significant amounts of data is also shown. R: segment length (m), S: number of segments.

0.52–0.60, which is a slightly smaller value than 0.65 reported in their paper. The distributions of filament sizes of cloudy and clear air are practically the same, suggesting that cloudy and clear air on average mix with the same proportion.

Next, we present results of box-counting analysis, a technique to estimate the fractal dimension of a set as described in detail by Feder (1988) or Falconer (1990). In essence, the space occupied by the investigated set is divided into a number of boxes of some size (in our case boxes are segments). If the number of boxes containing some elements of the set follows a power law as a function of box size, the exponent is the estimate of the fractal dimension of the set. This is the so-called box dimension D_B.

This analysis was applied to sets obtained in the way just described. In order to avoid edge effects due to record truncation, only boxes within record lengths were considered. Results of the box-counting analysis are presented in Fig. 3.

Cluster analysis is another technique of estimating the fractal dimension of a set (Feder 1988). In this technique the number M of set elements inside a circle of radius R centered on a chosen set element is counted and averaged for all center points. If $\bar{M}(R) \propto R^{D_c}$, D_c is an estimation of fractal dimension called cluster dimension.

This analysis was applied to the set defined by the cloud–clear air boundary points. Again, in order to avoid edge effects only circles of radius smaller than the distance to the edge of the data record were used. Results of the cluster analysis are presented in Fig. 4.

d. Results

The plots from the box counting and cluster analysis reveal scaling effects for a range of scales from several

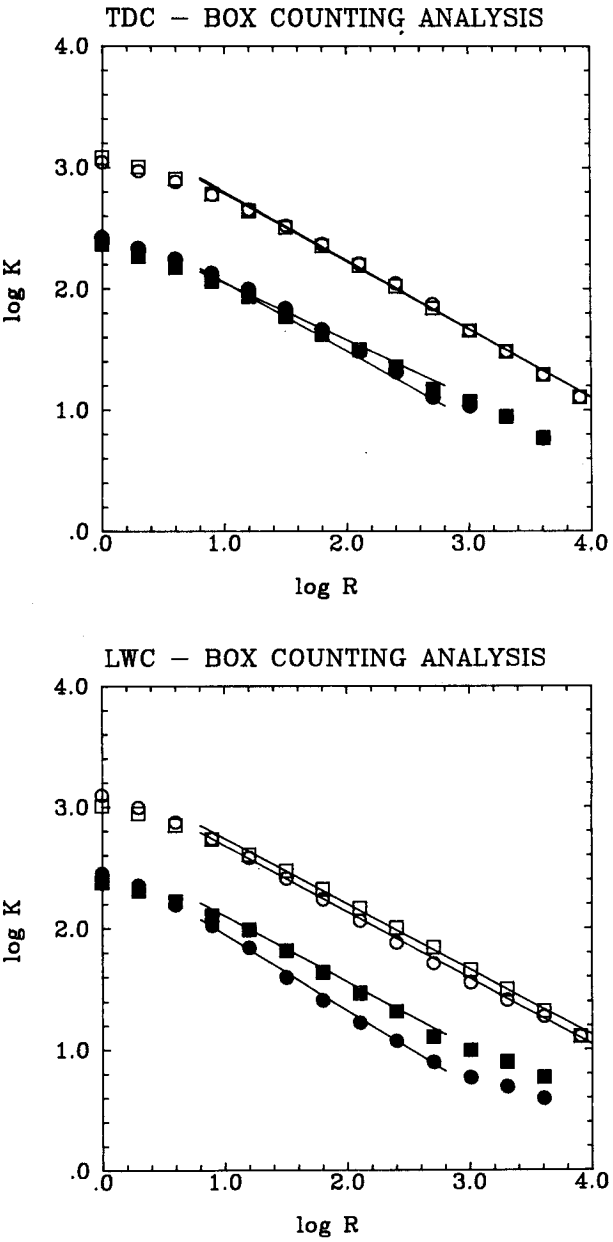

FIG. 3. Results of the box-counting analysis: (a) TDC, circles correspond to N_t = 10, squares to N_t = 150; (b) LWC, circles correspond to L_t = 0.1 g m^{-3}, squares to L_t = 0.5 g m^{-3}. Empty figures represent flight 42B, filled flight 44A. Best fit to the statistically significant points not affected by sampling resolution is also shown. K: number of boxes, R: box size (m).

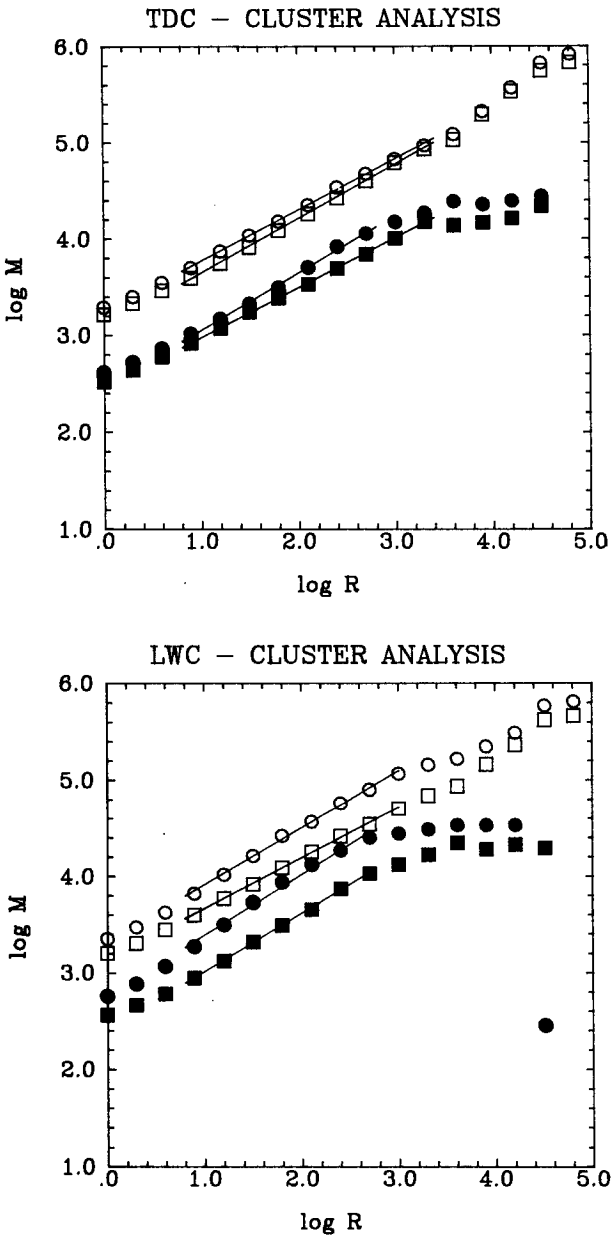

FIG. 4. Cluster analysis of the records. K: mean number of cloud–clear air border points in a circle, R: circle diameter (m). All other descriptions as on Fig. 3.

meters to thousands of meters. The scaling exponents are very close in all cases: for both TDC and LWC records and various thresholds of these quantities are used in the analysis. $D_1 = 0.55$ is an average in the mentioned range of scales, and according to (12) our estimate of the fractal dimension of the cloud surface is $D = 2.55$ with the standard deviation $\sigma = 0.04$. Error of the estimation, however, may be higher and dependent on the amount of points chosen to estimate slope of the straight line. There is no general rule for this choice and for the purpose of the current study only points forming straight line with a correlation above 0.997 were taken. Also, in the presence of gravity and buoyant forces the assumption of spatial isotropy on which (12) is based is questionable (Lovejoy and Schertzer 1986). Unfortunately, vertical cross sections through cumulus clouds, with sufficient resolution to check its validity, are not available.

Deviation of the experimental points from the straight line behavior at large scales may be attributed to statistically insufficient number of data. More important is the effect of curvature of the experimental points at the short scales (left-hand side of Figs. 3 and 4). For all of the analyses performed this curvature is toward smaller slopes (smaller D_1). This is an artificial effect attributable to the resolution of our experimental data. To prove this effect, an additional box-counting analysis was performed on data averaged over 2, 4, 8, and 16 samples, respectively. The results for the flight 42B TDC record and $N_t = 10$ are given in Fig. 5. As we can see, the curvature toward $D_1 = 0$ depends clearly on the averaging length and affects results of the box counting over a range of magnitude longer than the averaging length. This suggests that our estimated fractal dimension of the cloud–clear air interface may be valid for scales of order of 1 m and even smaller. Data of better resolution are needed, however, to prove this.

It is worthwhile to notice that the slope of the line in Fig. 2 (cumulative length distribution) is the same as D_1. This is not a general property of fractal sets. For

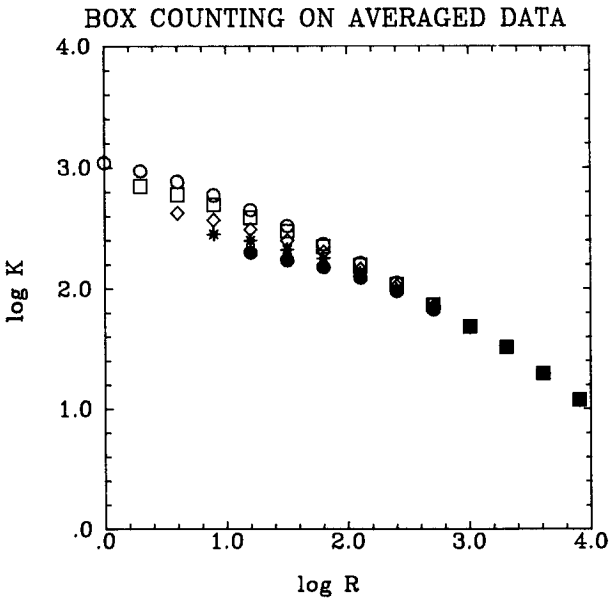

FIG. 5. Effect of averaging on the box-counting analysis for TDC data from flight 42B and for $N_t = 10$. Circles correspond to 64-Hz data (1-m averages), squares to 32 Hz (2-m averages), diamonds to 16 Hz (4 m), stars to 8 Hz (8 m), and dots to 4 Hz (16 m).

example, a triadic Cantor set has a fractal dimension $D_1 = \log 2/\log 3$, but the lengths of all of its "filaments" (segments forming the prefractal) is the same; that is, cumulative length distribution is the step function.

The fractal dimension obtained with thresholds between those described (i.e., $10 < \text{TDC} < 150$, $0.1 \text{ g m}^{-3} < \text{LWC} < 0.5 \text{ g m}^{-3}$) did not show any systematic changes with the threshold level, being very close to the average value of $D_1 = 0.55$ (see Table 2). This may indicate that the 1D horizontal cross section through cloud–clear air boundary behaves as a simple fractal. For high thresholds within the noisy level of the data (e.g., TDC = 240; see Fig. 1a) the dimension approaches unity. Thus, the rapid fluctuations near the adiabatic values appear to be close to random and seem to be generated by measurement errors due to small sampling volume of the FSSP.

TABLE 2. Estimated fractal dimension for cloud–clear air interface for two flights and different definitions of the interface (10 or 150 TDC, 0.1 g m^{-3} or 0.5 g m^{-3} LWC).

Threshold		D_{box}	D_{cor}
	Flight 42B		
N_t	10	2.53	2.57
	150	2.56	2.54
L_t	0.1 gm^{-3}	2.51	2.53
	0.5 gm^{-3}	2.57	2.59
	Flight 44A		
N_t	10	2.48	2.51
	150	2.55	2.59
L_t	0.1 gm^{-3}	2.55	2.58
	0.5 gm^{-3}	2.60	2.63

4. Discussion

The estimated value $D = 2.55$ of the fractal dimension of the cloud–clear air interface is significantly higher than the values given by SRM for shear flows, even when intermittence of the turbulent energy dissipation field is accounted for. On the other hand, our value corresponds well to the value given by CJ for fair weather cumuli of diameter over 500 m. The smaller value $D = 2.3$ for clouds of the diameter smaller than 500 m reported by CJ may be due to the effect of data resolution previously mentioned and illustrated in Fig. 5. The smallest pixel size of the satellite images used by CJ was 30 m and the estimate of the fractal dimension for clouds of diameters shorter than 500 m is probably affected by the data-resolution effect. Our result does not show any break in scaling properties at scales around 500 m.

The total droplet concentration in the first stages of cloud–environment mixing (before some drops evaporate completely) is a conservative quantity, similar to the concentration of the passive scalars used by SRM in their measurements. The difference in the fractal dimension obtained for surfaces of constant droplet concentration in clouds and the one given by SRM for shear-flow turbulence may be due to the different mechanisms that generate the two types of turbulent motions. As suggested by Grabowski and Clark (1991), the turbulence on the cloud edge and the resulting convolution of the cloud surface are driven by baroclinic instability in a narrow zone along the cloud boundary. That is, the production of the turbulent energy occurs in a narrow region, evolving during development of convolutions. This driving mechanism is different from the one producing turbulence in shear flows and may cause the different values in fractal dimension of the interfaces. This difference has a tremendous effect on the estimates of the characteristic properties of the mixing process given in Table 1. As we can see, the new characteristic size of the filaments, assuming initial size of the mixing event $L = 100$ m, is in the range 10–20 cm, below the resolution of the experimental data. The fraction of the well-mixed air during this phase is still very small. Expression (11) now gives a much more reasonable value of t_2 within the range of one hour.

Characteristic size of the initial engulfment on the cloud–clear air interface $L = 100$ m was taken after Grabowski and Clark (1991) for our estimates. However, as one can see on Figs. 2, 3, and 4, this does not imply that 100 m is a preferred scale for cloud–environment mixing process, and initial convolutions of different sizes are likely. In fact, in the entire range of the examined experimental data a preferred scale does not appear.

It has been suggested by Sreenivasan (private communication) that once the large-scale engulfment takes place and the first step of the mixing has occurred, the surface across which diffusion takes place in the second stage is no longer the cloud boundary, but an internal boundary (Constantin et al. 1991). According to theory and some experimental tank measurements, such an internal boundary has dimension 2.67, closer to our measured value. The question arises, then, as to whether such an internal surface is not responsible for our dimension values to be between 2.35 and 2.67. We do not think this is the case. In our observations scaling extends continuously up to 10-km scales with dimension value practically independent of threshold. We should not expect the internal boundary to extend to these scales. On the other hand, simple numerical experiments with Cantor sets in which the dimension is changed during the cascading process show that box-counting analysis (such as on Fig. 3a) leads to lines broken at the scale where the cascading law was changed. Moreover, using dimension 2.67 gives t_2 of the same order as t_1. Thus, the dissipation of clouds would take place in time of order of few minutes, con-

trary to experience. It appears to us that the difference in the mechanisms generating the turbulence is the more likely explanation for the difference in our dimension value as compared to the laboratory experiment with nonstratified, nonreacting, well-developed shear flows.

All of the entrainment–mixing estimations presented here were made under the assumption that droplet sedimentation may be negligible. Obviously this assumption is very crude and does not reflect the real situation at small scales (10 cm and less). Droplet sedimentation certainly will affect the clear picture of entrainment–mixing process in its second stage. The effect will be stronger for higher LWC and bigger droplets, observed in well-developed cumulus clouds. However, our estimates of the fractal dimension show that the entrainment–mixing process in clouds differs from similar processes in shear flows not only by the transport mechanism through interfaces, but also by different geometry of these interfaces.

Jensen and Baker (1989) suggest that mixing within clouds is neither extremely homogeneous nor extremely inhomogeneous. Due to the adopted BB approach, they do not take into account the presence of filaments of the whole range of scales and, consequently, consider mixing to be uniform in space. However, if one assumes that the cloud–environment interface has fractal properties in a wide range of scales and the intermittence of the turbulent energy has the fractal structure with remarkable singularities as well (SPMR), a different picture of the mixing process appears. Some parts of the mixing event undergo fast, homogeneous mixing, while other may remain unmixed for a relatively long time or are mixed with different volumes of cloudy, environmental or previously mixed air, which is a quite nonuniform mixing process. Thus, mixing is neither homogeneous nor inhomogeneous, and at the same time has rather spotty structure, with patches of different levels of homogeneity. Some extreme spots are likely to be present. If the fractal structure of the interface is confirmed to occur in well-developed cumulus clouds, this result may have consequences on the formation of the big droplets responsible for the eventual development of precipitation.

Acknowledgments. The experimental data used for the analysis were obtained from the Atmospheric Environment Service courtesy of Dr. George Isaac. We thank Dr. Graciela Raga and Dr. Walter Strapp for help in selecting and extracting data from the database. Discussions with Dr. Antoine Saucier gave us a deeper insight into the field of fractal geometry and its application to fluid mechanics. Remarks by Dr. Wojciech Grabowski and Dr. Peter Zwack after proofreading the paper significantly raised its quality. Reviewers' suggestions helped to omit some drawbacks and to extend discussion of our results.

This research was partially supported by a grant from the Atmospheric Environment Service.

REFERENCES

Austin, P. H., M. B. Baker, A. M. Blyth, and J. B. Jensen, 1985: Small-scale variability in warm continental cumulus clouds. *J. Atmos. Sci.*, **42,** 1123–1138.

Broadwell, J. E., and R. E. Breidenthal, 1982: A simple model of mixing and chemical reaction in turbulent shear layer. *J. Fluid Mech.*, **125,** 397–410.

Brown, G. L., and A. Roshko, 1974: On density and large structure in turbulent mixing layers. *J. Fluid Mech.*, **64,** 775.

Cahalan, R. R., and J. H. Joseph, 1989: Fractal statistics of cloud fields. *Mon. Wea. Rev.*, **117,** 261–272.

Carter, P. H., R. Cawley, A. L. Licht, J. A. Yorke, and M. S. Melnik, 1986: Dimension measurements from cloud radiance. *Dimensions and Entropies in Chaotic Systems,* G. Mayer-Kress, Ed., Springer, 215–221.

Constantin, P., I. Procaccia, and K. R. Sreenivasan, 1991: Fractal geometry of isoscalar surfaces in turbulence: Theory and experiments. *Phys. Rev. Lett.*, **67,** 1739–1742.

Duroure, C., and B. Guillemet, 1990: Analyse des heterogeneites spatiales des Stratocumulus et Cumulus. *Atmos. Res.*, **25,** 331–350.

Falconer, K., 1990: Fractal geometry. *Mathematical Foundations and Applications,* Wiley & Sons, 288 pp.

Feder, J., 1988: *Fractals.* Plenum, 283 pp.

Gifford, F. A., 1989: The shape of large tropospheric clouds, or "very like a whale." *Bull. Amer. Meteor. Soc.*, **70,** 468–475.

Grabowski, W. W., and T. L. Clark, 1991: Cloud–environment interface instability: Rising thermal calculations in two spatial dimensions. *J. Atmos. Sci.*, **48,** 527–546.

Jensen, J. B., and M. B. Baker, 1989: A simple model of droplet spectral evolution during turbulent mixing. *J. Atmos. Sci.*, **46,** 2812–2829.

Lovejoy, S., 1982: Area–perimeter relation for rain and cloud areas. *Science,* **216,** 185–187.

——, and D. Schertzer, 1986: Scale invariance, symmetries, fractals and stochastic symulations of atmospheric phenomena. *Bull. Amer. Meteor. Soc.*, **67,** 21–32.

MacPherson, J. I., 1979: A comparison of turbulent characteristics of cumulus clouds measured near Yellowknife and Thunder Bay. *DME/NAE Quart. Bull.*, 1979(1), 38 pp.

——, and G. A. Isaac, 1977: Turbulent characteristics of some Canadian cumulus clouds. *J. Appl. Meteor.*, **16,** 81–90.

Mandelbrot, B. B., 1982: *The Fractal Geometry of Nature.* W. H. Freeman, 468 pp.

Paluch, I. R., and D. G. Baumgardner, 1989: Entrainment and fine scale mixing in a continental convective cloud. *J. Atmos. Sci.*, **46,** 261–278.

Sreenivasan, K. R., and C. Menevau, 1986: Fractal facets of turbulence. *J. Fluid Mech.*, **173,** 357–386.

——, R. Ramshankar, and C. Menevau, 1989a: Mixing, entrainment and fractal dimensions of surfaces in turbulent flows. *Proc. Roy. Soc. Lond.* **A421,** 79–108.

——, R. R. Prasad, C. Menevau, and R. Ramshankar, 1989b: The turbulent geometry of interfaces and multifractal distribution of dissipation in fully turbulent flows. *Pure Appl. Geophys.*, **131,** 43–60.

Turner, J. S., 1986: Turbulent entrainment: The development of the entrainment assumption, and its application to geophysical flows. *J. Fluid Mech.*, **173,** 431–471.